Determination of postexcitation thresholds for single ultrasound contrast agent microbubbles using double passive cavitation detection

Daniel A. King[a)]
Department of Mechanical Science and Engineering, University of Illinois at Urbana-Champaign, 1206 W. Green Street, Urbana, Illinois 61801

Michael J. Malloy, Alayna C. Roberts, Alexander Haak, Christian C. Yoder, and William D. O'Brien, Jr.
Department of Electrical and Computer Engineering, Bioacoustics Research Laboratory, University of Illinois at Urbana-Champaign, 405 North Mathews, Urbana, Illinois 61801

This work presents experimental responses of single ultrasound contrast agents to short, large amplitude pulses, characterized using double passive cavitation detection. In this technique, two matched, focused receive transducers were aligned orthogonally to capture the acoustic response of a microbubble from within the overlapping confocal region. The microbubbles were categorized according to a classification scheme based on the presence or absence of postexcitation signals, which are secondary broadband spikes following the principle oscillatory response of the ultrasound contrast agent and are indicative of the transient collapse of the microbubble. Experiments were conducted varying insonifying frequencies (0.9, 2.8, 4.6, and 7.1 MHz) and peak rarefactional pressures (200 kPa to 6.2 MPa) for two types of contrast agents (Definity® and Optison™). Results were fit using logistic regression analysis to define pressure thresholds where at least 5% and 50% of the microbubble populations collapsed for each frequency. These thresholds were found to occur at lower pressures for Definity than for Optison over the range of frequencies studied; additionally, the thresholds occurred at lower pressures with lower frequencies for both microbubble types in most cases, though this trend did not follow a mechanical index scaling.
© 2010 Acoustical Society of America. [DOI: 10.1121/1.3373405]

I. INTRODUCTION

Ultrasound contrast agents (UCAs) are thin-shelled microbubbles with a gas core typically ranging in diameter from $1-10$ μm. While the current clinical usage of UCAs is primarily their enhancement of imaging in diagnostic ultrasound, specifically for contrast echocardiography,[1,2] much of the focus of recent research has shifted to the therapeutic potential of UCAs used in conjunction with ultrasound. Among other procedures, recent experimental studies have shown that use of UCAs in conjunction with ultrasound enhances thrombolysis,[3,4] sonoporation across cellular membranes,[5–7] and molecular transport across the blood brain barrier.[8–10]

UCAs have been shown to be successful in increasing the effectiveness of such therapies, but the precise physical mechanisms leading to these bioeffects remain inadequately explained. In response to an ultrasonic pressure field, UCAs may undergo a wide range of dynamic responses ranging from linear oscillation to transient inertial collapse and fragmentation.[11,12] However, cavitation responses for different types of shelled microbubbles in reaction to large amplitude pulses are insufficiently documented. Greater under-standing of microbubbles undergoing large amplitude oscillatory behavior, including the experimental determination of accurate collapse thresholds, will lead both to improved modeling of shelled bubble dynamics and also elucidation of the physical mechanisms for bioeffects resulting from functional usage of UCAs.

Experimental methods to characterize microbubble response generally fit into two categories, optic and acoustic. Optical observations are usually considered the standard by which microbubble responses are judged due to their ability to distinguish initial conditions of the microbubble as well as radial expansion and compression. While the majority of optical studies focus on small amplitude UCA responses, several studies have examined behaviors associated with the destruction of UCAs due to large amplitude pulses, including fragmentation, gas release, and rebound.[13–15] Optical studies provide valuable insight into microbubble behavior, but there are also drawbacks to this approach including limited temporal and spatial resolution, limited size of the data set, and expense involved in the necessary equipment.[16]

For these reasons, as well as for potential use *in vivo*,[17] acoustic approaches for monitoring microbubble activity are appealing. Acoustic studies can be divided into two subcategories: active cavitation detection (ACD) and passive cavitation detection (PCD). ACD uses a secondary low pressure pulse to investigate changes caused by the initial pulse.[18,19]

---

a)Author to whom correspondence should be addressed. Electronic mail: daking3@illinois.edu

However, while the measurement pulse in ACD has significantly less energy than the primary pulse, it still has the potential to affect the cavitation process.[20] In contrast, passive cavitation detection only involves listening to the response. The primary challenge with acoustic studies lies in signal interpretation, and this has led to a wide variety of approaches. One PCD study defined the UCA fragmentation threshold as the pressure level at which 5% or more of the spikes in the time trace exceeded a specified voltage threshold, and simultaneously defined the inertial cavitation (IC) threshold as a sudden increase in broadband noise in the frequency spectrum.[21] Other studies have defined the IC threshold as an increase in broadband noise of one standard deviation greater than the background noise,[22] a sudden spectral power increase of at least 20 dB above the background noise,[23] or simply as a qualitatively different signal that disappears after a single tone burst.[18] It is generally agreed that a large amplitude UCA response, such as is involved with inertial cavitation or microbubble fragmentation, is also associated with some amount of increase in broadband spectral content; however, the definitions found in literature are often qualitative and arbitrary.

Previous work related to the current study proposed using passive cavitation detection to monitor microbubble destruction based on the relationship of two characteristic features of the acquired temporal signals: the principle response, defined as the initial harmonic response of the microbubble lasting in duration up to the length of the transmitted pulse, and the presence or absence of a postexcitation signal (PES), defined as a secondary broadband response separated in time from the principle response—typically $1-5$ μs later.[24] In this work, it is hypothesized that this type of rebound signal only occurs for free (unshelled) gas bubbles emitted during rebound of the UCA and consequently is linked to shell rupture and transient collapse of the UCA. This categorization approach for characterizing UCA responses is attractive for being, in principle, a non-arbitrary definition of transient microbubble collapse activity.

These postexcitation signals are consistent with examples of free bubble rebound and re-collapse that have been observed in numerous situations with larger bubbles; for example, in simultaneous optic and PCD lithotripsy experiments[25] and during sonoluminescence.[26] The Marmottant model[27] predicts that both microbubble shell rupture and expansion beyond the inertial cavitation threshold, defined as twice the initial radius, are necessary conditions for postexcitation; additionally, presence of postexcitation rebound has been associated with an increase in broadband content, demonstrating a relationship with the strength of the inertial collapse.[28] While the survival of microbubbles without postexcitation is unclear, numerous previous observations such as these solidly link postexcitation with the transient collapse of the UCA microbubble.

Using a single focused receive PCD transducer on isolated UCAs has been found to be able to determine minimum destruction thresholds of isolated, unconstrained microbubbles.[29] However, due to variability in the spatial location of the microbubble relative to the focus of the incident pulse, previous studies were generally unable to establish any ob-
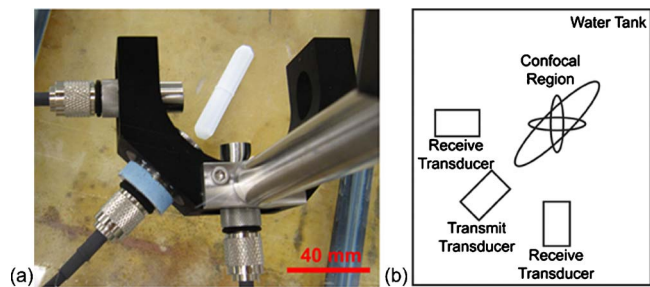

FIG. 1. (Color online) (a) Photograph and (b) schematic of the experimental setup.

vious trend between the amount of microbubble collapse and the peak rarefactional pressure amplitude (PRPA), a relationship which might be expected for a robust measure of cavitation activity. To address the challenge of determining spatial location, the current work utilized two matched receive transducers to limit the confocal region from which acceptable responses were obtained.

Double passive cavitation detection of UCAs using two receive transducers with different center frequencies has been previously reported.[30] However, that particular experimental setup only allowed for imprecise comparisons between the two received signals due to the differences in the transducers. The current double PCD study avoids these limitations by using matched high frequency receive transducers, thereby reducing both spatial uncertainty of the microbubble and incidence of asymmetrical behavior potentially occurring from interactions with surrounding microbubbles.

II. MATERIALS AND METHODS

A. Data collection

The setup for the double passive cavitation detection system involved the confocal alignment of three single element transducers (Valpey Fisher, Hopkinton, MA). Two passive receive transducers were placed at a 90° angle with one active transmit transducer positioned at an angle of 45° between them (Fig. 1). Alignment of the transducers was performed using a 50 μm diameter wire; the fields of all transducers were also characterized using this wire technique and the -6 dB beamwidths of the receive transducers were 0.27 mm (Fig. 2).[31] The center frequencies of the two receive transducers were nominally 15 MHz, but measured to be 14.6 and 13.8 MHz in pulse-echo mode; both were $f/2$, with an element diameter of 0.5″. The center frequencies of the four transducers used to generate the transmitted pulse were 0.95, 2.8, 4.6, and 7.1 MHz; all were $f/2$, with an element diameter of 0.75″.

Three cycle tone bursts with a pulse repetition frequency of 10 Hz at the center frequency of each transmit transducer were generated using a pulser-receiver system (RITEC RAM5000, Warwick, RI). An attenuation bar (Model 358, Arenberg Ultrasonic Laboratory, Boston, MA) was used to achieve the lowest pressure settings. To determine the pressure amplitudes of the generated waveforms, all settings were calibrated using a PVDF hydrophone (0.5 mm diam-
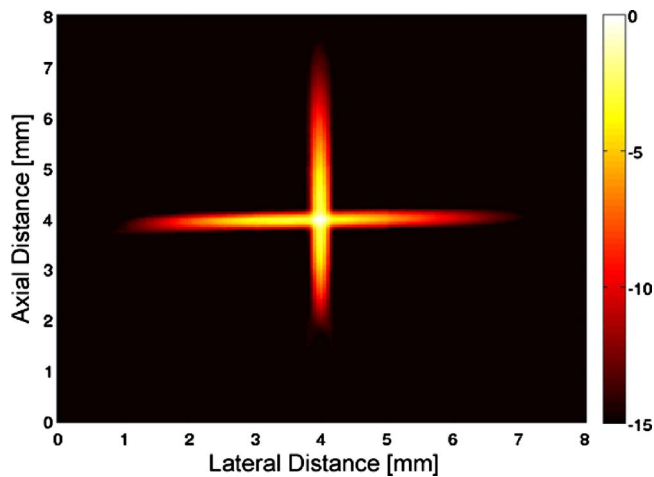
FIG. 2. (Color online) Measured overlapping confocal region of the receive transducers, formed by overlaying the pulse intensity integral obtained using the wire characterization technique of each aligned receiver. The color scale is in dB.

eter, Marconi 6999/1/00001/100; GEC Marconi Ltd., Great Baddow, U.K.) at the center of the confocal region of the receive transducers according to established procedures.[32,33]

The two commercial contrast agents used in these experiments were lipid-shelled Definity® (Lantheus Medical Imaging, N. Billerica, MA) and albumin-shelled Optison™ (GE Healthcare Inc., Princeton, NJ). The reported mean diameter range of Definity is 1.1 to 3.3 μm, with 98% having a diameter less than 10 μm; the maximum initial concentration is 1.2×10^{10} microspheres/ml. The reported mean diameter range of Optison is 3.0 to 4.5 μm, with 95% having a diameter less than 10 μm; the initial concentration is 5 to 8×10^8 microspheres/ml. Both types of microbubbles contain octafluoropropane as the gas core. Since each experimental trial used only a small amount of contrast agents, vials were reused for several trials. Prior to each experiment, the contrast agents were re-activated according to package instructions. They were diluted to less than one bubble per confocal volume (approximately 5000 bubbles/ml) upon being added to the water tank.

The transducer holder was placed in a Plexiglas tank filled with 15 to 25 L of degassed water at a temperature between 20 °C to 22 °C. Prior to the addition of microbubbles in the water tank, 50 signals were collected to determine the experimental system noise for each trial. Noise levels were determined by binning the amplitude of each sample, assuming Gaussian noise, and setting the required signal threshold greater than 3.29 standard deviations from the mean. This is equivalent to a noise limit set at 0.1% of the absolute value maximum obtained in these control signals. The appropriate concentration of UCAs was then added and the mixture was gently stirred with a magnetic stir bar to ensure uniformity of the UCA distribution. Loss of acoustically active microbubbles in each trial occurred due to buoyancy and also due to gas diffusion across the shelled surface.[34] Therefore, microbubbles were replenished approximately every 5–7 min when the rate of observable events decreased noticeably. In a typical experiment, several thousand signals at each pressure level were acquired continuously; the total experimental time was less than 45 min following initial activation of the UCAs.

Signals acquired by the receive transducers were amplified by 22 dB, digitized using an A/D converter (12-bit, 200 MS/s, Strategic Test digitizing board UF 3025, Cambridge, MA), and saved to a PC for offline processing using MATLAB® (The Math Works, Inc., Natick, MA). The signals were processed to remove the DC component from the signal and then low pass filtered with cutoff frequency 20 MHz to remove excessive system noise frequencies.

B. Data analysis

While the concentration of UCAs was chosen such that there should have been approximately one microbubble per confocal volume on average, this does not preclude the possibility that there were greater or fewer than one microbubble present in the receiving region at any given time. Therefore, the received signals must be classified to eliminate those which do not contain a single bubble. Seven categories were used for classification: (1) no bubbles within the receiving region, (2) multiple bubbles within the receiving region, (3) a single bubble out of the confocal region, (4) a single bubble with postexcitation signals (PES) in only one channel, (5) a single bubble with PES in both channels, (6) a single bubble with no PES, or (7) unknown.

A large majority of the total acquired signals were not used in the final analysis, which is expected since the total receiving region is larger and more likely to contain microbubbles than the desired overlapping confocal region. Approximately 80% to 90% of the data set was automatically classified in one of the first three categories and was immediately rejected from further analysis. Signals with no samples in either channel greater than the predetermined noise limits were classified as category 1, no bubbles within the receiving region. Signals where the duration of the envelope exceeding the signal threshold in either channel was 3 times that of the transmitted pulse length were classified as category 2, multiple bubbles within the confocal region. Category 3, a single bubble out of the confocal region, was defined as signals where the difference in time of arrival determined through cross-correlation of the two channels exceeded 1 μs, or where the amplitude of the response in one channel exceeded five times that in the second channel [Fig. 3(a)]. Both of these criteria are indicative of a signal source location significantly closer to one receive transducer than the other, which is outside the confocal region.

The remaining signals were classified through visual analysis of both the voltage-time signal and frequency-time spectrogram calculated with a sliding Hanning window (1.28 μs, in steps of 0.02 μs). Additional signals which did not satisfy the above criteria were nonetheless identified as belonging to one of the first three categories, leaving approximately 10% to 40% of the manually classified signals categorized as containing a single microbubble within the confocal region. Category 4, a single bubble containing PES in only one channel, was also removed from analysis on the basis that such bubbles were responding with non-spherically

J. Acoust. Soc. Am., Vol. 127, No. 6, June 2010

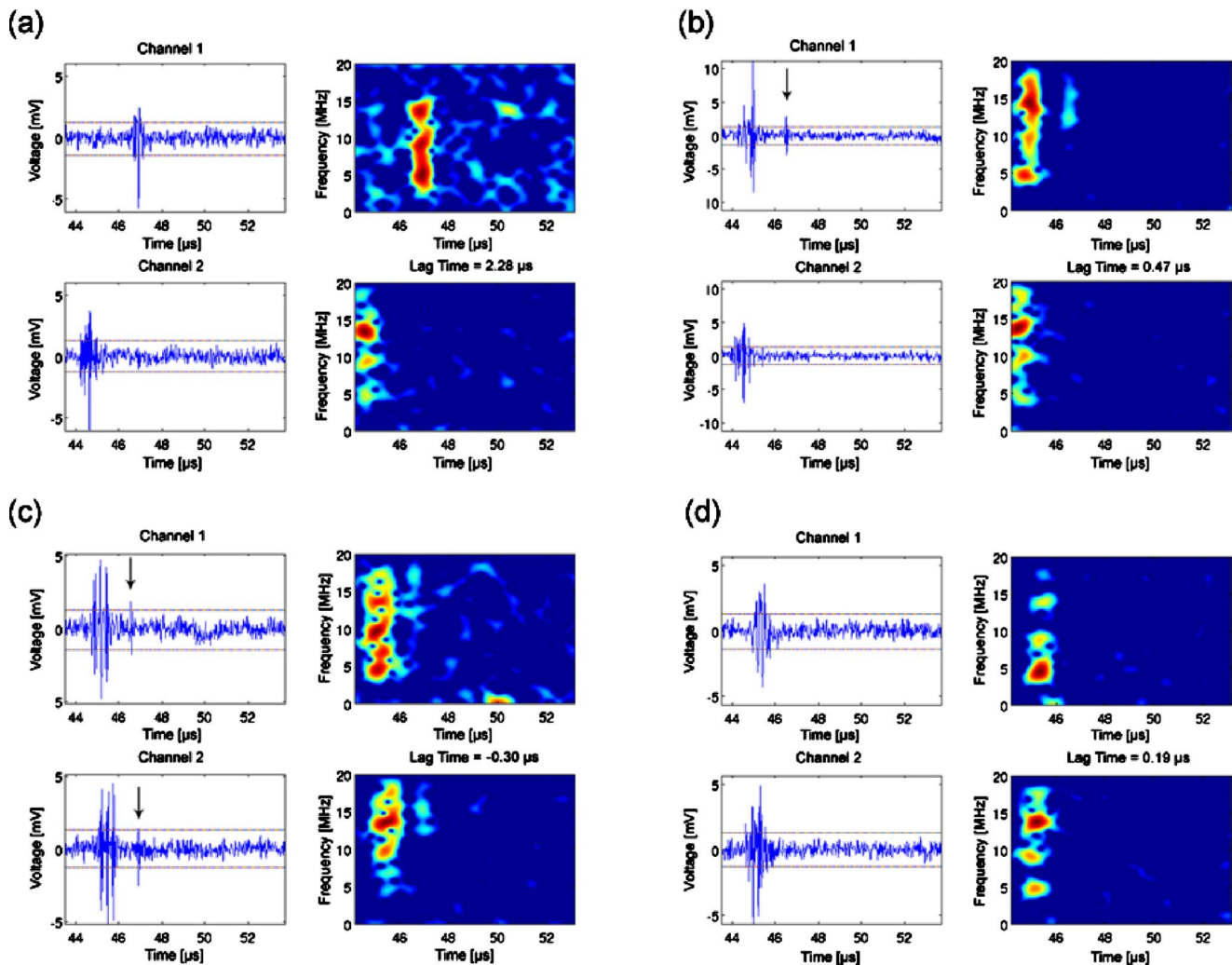King et al.: Contrast agent postexcitation thresholds   3451

FIG. 3. (Color online) Example of voltage-time (right column) and corresponding frequency-time (left column) signals at 4.6 MHz and PRPA 4.47 MPa. Signal thresholds are shown as horizontal lines on the voltage-time plots. (a) Single bubble out of confocal region due to time lag between signals. (b) Single bubble with postexcitation (marked with an arrow) only observable in channel 1. (c) Single bubble with postexcitation in both receive channels. (d) Single bubble with no postexcitation, only the principle response, in both receive channels.

symmetric behavior and therefore may have been influenced by proximity to other nearby bubbles [Fig. 3(b)]. Finally, signals in which the occurrence of a principle response or PES was unclear, category 7, were also eliminated from the final analysis. Only those categories clearly containing a single bubble within the confocal region and clearly exhibiting symmetric behavior, categories 5 and 6 [Figs. 3(c) and 3(d)], were used for subsequent statistical analysis.

Since the final classification is done manually, there will inherently be some variability in what determined to be a postexcitation or non-postexcitation signal; nevertheless, the overall trend of increasing postexcitation with increasing PRPA for each classifier was clear and consistent. Three persons with varying levels of familiarity to the project were trained to classify the experimental data; the average number of single bubble signals with or without PES used for analysis per unique pressure and frequency settings for Definity and Optison were 30 ($\pm$9) and 20 ($\pm$8), respectively.

C. Logistic curve fitting

A percentage postexcitation threshold is defined as the level at which a certain percentage of the total population of

microbubbles transiently collapses with PES. For example, a 5% threshold will occur near the inception of PES. To determine these thresholds from the experimental data, the number of signals exhibiting PES divided by the total number of single bubble signals (not including category 4 responses)
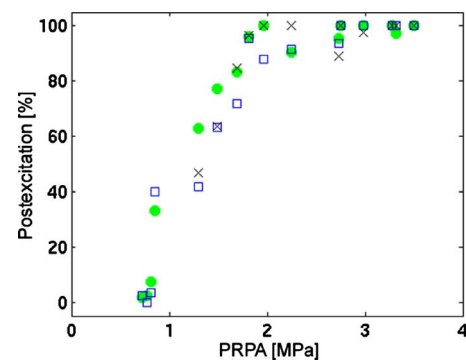

FIG. 4. (Color online) Percentage postexcitation determined by three individual classifiers plotted against peak rarefactional pressure for Definity UCAs at 2.8 MHz. The average number of signals per data point per classifier (mean $\pm$ standard deviation) is 34 $\pm$ 11.
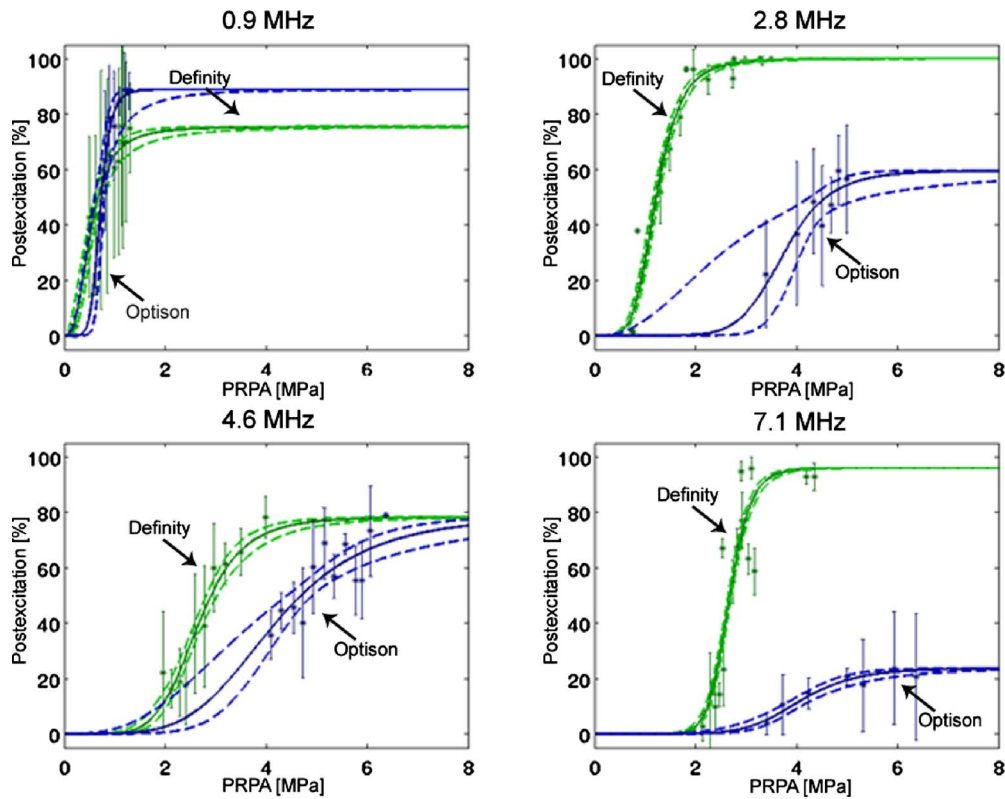
King et al.: Contrast agent postexcitation thresholds

FIG. 5. (Color online) Percentage postexcitation curves for Definity and Optison UCAs, plotted against PRPA and grouped by frequency. The asterisks (*) represent averages plotted with standard deviations from three persons who classified the experimental data. The solid (–) curve is the logistic fit, and the dotted (- -) curves represent the 95% confidence intervals. The average number of signals per data point (mean ± standard deviation) is 30 ± 9 for Definity and 20 ± 8 for Optison.

was fit with a curve using PRPA as the independent variable. It was observed in most cases that the percentage of postexcitation increased from a minimum to a maximum value which was usually less than 100%. Therefore, the resulting averages from three independent classifications were fit with a modified logistic regression curve [Eq. (1)], beginning at zero for zero acoustic pressure and increasing to the maximum observed percentage of PES.

$$P(z) = \frac{Qe^{\alpha_0 + \alpha_1 z}}{1 + e^{\alpha_0 + \alpha_1 z}}. \tag{1}$$

Here, $P(z)$ is the percentage of collapse, z is the log transform of the PRPA, Q is the maximum observed percentage of PES ($0 \leq Q \leq 1$), and α_0 and α_1 are the fitting coefficients. This curve determines the amount of postexcitation present at a certain PRPA proportional to the maximum amount observed for a specific frequency, and is used as a metric for comparing similar relative amounts of cavitation activity across different insonifying conditions.

III. RESULTS

The three individual classifications for Definity UCAs at 2.8 MHz are presented in Fig. 4. This example demonstrates the major features of the classification analysis as described above; at the lowest peak rarefactional pressures where single UCA signals were able to be identified, little to no postexcitation is observed. As PRPA is increased, the per-

centage of PES relative to the total number of individual microbubble signals also increases—in this instance, to a maximum at 100%.

The classification results for all four frequencies and both microbubble types are presented as mean ± standard deviation from the three individual classifiers in Fig. 5. Additionally, the logistic curve fits to these averages and 95% confidence interval regions are shown. The maximum observed percentage of postexcitation for Definity UCAs ranges from approximately 70% to 100%, while this maximum for Optison is lower in most cases, ranging from approximately 20% to 90%.

Specific percentage postexcitation thresholds proportional to the maximum at each frequency are also determined from the logistic curves. Results for the 5% and 50% thresholds are listed in Table I, along with their corresponding 95% confidence intervals. As frequency is increased for each type of UCA, the PRPA required to reach a specified threshold increases in most instances. The PRPA values for these thresholds are also consistently lower for Definity than for Optison, indicating that for an insonation at a specified frequency with a high enough PRPA, the Definity bubble population undergoes greater postexcitation activity.

IV. DISCUSSION AND CONCLUSIONS

In this study, double passive cavitation detection was successfully applied to single ultrasound contrast agents to identify the presence or absence of a postexcitation signal.

J. Acoust. Soc. Am., Vol. 127, No. 6, June 2010

King *et al.*: Contrast agent postexcitation thresholds   3453

TABLE I. Percentage postexcitation thresholds with 95% confidence intervals in MPa PRPA, proportional to the maximum postexcitation observed at each frequency.

Frequency (MHz)	Definity		Optison	
	5%	50%	5%	50%
0.9	0.19 (0.12–0.26)	0.54 (0.46–0.60)	0.47 (0.19–0.59)	0.72 (0.56–0.78)
2.8	0.68 (0.62–0.74)	1.22 (1.17–1.28)	2.62 (0.76–3.27)	3.75 (2.53–4.09)
4.6	1.63 (1.45–1.77)	2.65 (2.57–2.74)	2.20 (1.32–2.75)	4.17 (3.67–4.40)
7.1	2.10 (2.03–2.16)	2.67 (2.64–2.70)	2.73 (2.27–3.02)	4.07 (3.87–4.28)

By reducing spatial variability in the location of the analyzed microbubbles with two matched receive transducers, a clear relationship between postexcitation occurrence and peak rarefactional pressure of the incident pulse is observed. The observed trends of greater cavitation activity at higher pressures and at lower frequencies for both types of microbubbles in this experiment are consistent with other experimental results of ultrasound contrast agent collapse.[13,14,19,21]

The PES threshold behavior was significantly different between Definity and Optison. The primary physical distinctions between the two types of UCAs are size distribution and shell composition, both of which may contribute to measured differences in thresholds and in maximum observed levels of PES. Bubble rebound will likely involve fragmentation of the gas content during transient collapse of the UCA. It has been observed both experimentally[35] and theoretically[36] that if the fragmentation of the bubble is such that the gas content is not of a critical size, it diffuses into the liquid without a violent rebound. Thus, it may be expected that while the PES is indicative of shell rupture and transient collapse of the bubble, the converse may not always be true even when the experimental conditions are designed to capture a spherically symmetric response. While postexcitation is indicative of transient collapse, the potential for destruction of UCAs not involving PES suggests these reported thresholds should be considered lower bounds on the percentage of UCAs being irreversibly altered.
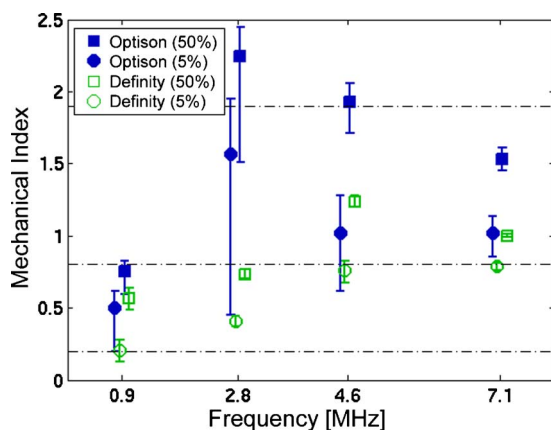

FIG. 6. (Color online) Postexcitation thresholds and 95% confidence intervals at 5% (circles) and 50% (squares), plotted versus frequency on the mechanical index scale. Definity is plotted with open symbols, and Optison is plotted with closed symbols. Low, moderate, high, and above regulatory limit regimes are indicated with the horizontal dashed-dotted (–.) lines.

The mechanical index (MI) is commonly used to gauge the likelihood of biomechanical effects due to cavitation activity from ultrasound, and the short pulse length and low duty cycle parameters used in this double PCD experiment are within the requirements for its applicability. According to this theory, acoustic insonations related by Eq. (2) may result in similar cavitation activity.[37,38]

$$MI = \frac{PRPA[MPa]}{\sqrt{f}[MHz]}. \tag{2}$$

To compare the postexcitation cavitation results with the mechanical index, the PES thresholds and 95% confidence intervals listed in Table I are plotted on the MI scale (Fig. 6). A mechanical index around 0.1 is considered low MI, 0.2–0.7 is considered moderate MI, and above 0.8 is considered high MI, with an FDA regulatory limit of 1.9.[39] The double PCD results show that postexcitation activity of these UCAs is particularly divergent from the MI scaling at the two lowest frequencies tested. Large percentages (50% and greater) of the populations of both types of microbubbles exhibit postexcitation at moderate MI levels for the lowest frequency tested, 0.9 MHz; at higher frequencies, Definity also undergoes PES activity within moderate MI, while Optison requires higher MI to achieve similar levels of PES activity at these higher frequencies. The lack of agreement with MI scaling adds to evidence that MI is an inadequate predictor of UCA cavitation activity.[39]

The response of an ultrasound contrast agent due to an ultrasonic pulse is dependent on material properties of the shell and gas core as well as the size of the microbubble. The occurrence of postexcitation, as an indicator of transient collapse cavitation activity, reflects physical variations in individual UCAs. While Definity and Optison both contain the same gas, they are composed of different shell materials and have different size ranges as well. Additional studies where these parameters are controlled independently of one another would be necessary to determine which has the greatest impact on occurrence of PES and therefore explain the observed variations in thresholds between microbubbles with different properties.

ACKNOWLEDGMENTS

[1]K. Wei and S. Kaul, "Recent advances in myocardial contrast echocardiography," Curr. Opin. Cardiol. **12**, 539–546 (1997).

[2]S. L. Mulvagh, H. Rakowski, M. A. Vannan, S. S. Abdelmoneim, H. Becher, S. M. Bierig, P. N. Burns, R. Castello, P. D. Coon, M. E. Hagen, J. G. Jollis, T. R. Kimball, D. W. Kitzman, I. Kronzon, A. J. Labovitz, R. M. Lang, J. Mathew, W. S. Moir, S. F. Nagueh, A. S. Pearlman, J. E. Perez, T. R. Porter, J. Rosenbloom, G. M. Strachan, S. Thanigaraj, K. Wei, A. Woo, E. H. Yu, and W. A. Zoghbi, "American Society of Echocardiography consensus statement on the clinical applications of ultrasonic contrast agents in echocardiography," J. Am. Soc. Echocardiogr **21**, 1179–1201 (2008).

[3]S. Datta, C. C. Coussios, A. Y. Ammi, T. D. Mast, G. M. de Courten-Myers, and C. K. Holland, "Ultrasound enhanced thrombolysis using Definity as a cavitation nucleation agent," Ultrasound Med. Biol. **34**, 1421–1433 (2008).

[4]W. T. Shi, J. E. Powers, A. L. Klibanov, and C. S. Hall, "In-vitro investigation of thrombosis dissolution with microbubble induced continuous acoustic activities," in Proceedings of the IEEE Ultrasonics Symposium Proceedings:1985–1988 (2007).

[5]M. Ward, J. Wu, and J. F. Chiu, "Ultrasound-induced cell lysis and sonoporation enhanced by contrast agents," J. Acoust. Soc. Am. **105**, 2951–2957 (1999).

[6]A. van Wamel, K. Kooiman, M. Harteveld, M. Emmer, F. J. ten Cate, M. Verslius, and N. de Jong, "Vibrating microbubbles poking individual cells: Drug transfer into cells via sonoporation," J. Controlled Release **112**, 149–155 (2006).

[7]M. M. Forbes, R. L. Steinberg, and W. D. O'Brien, Jr., "Examination of inertial cavitation of Optison in producing sonoporation of Chinese hamster ovary cells," Ultrasound Med. Biol. **34**, 2009–2018 (2008).

[8]N. McDannold, N. Vykhodtseva, and K. Hynynen, "Targeted disruption of the blood–brain barrier with focused ultrasound: Association with cavitation activity," Phys. Med. Biol. **51**, 793–807 (2006).

[9]J. J. Choi, M. Pernot, T. R. Brown, S. A. Small, and E. E. Konofagou, "Spatio-temporal analysis of molecular delivery through the blood brain barrier using focused ultrasound," Phys. Med. Biol. **52**, 5509–5530 (2007).

[10]N. McDannold, N. Vykhodtseva, and K. Hynynen, "Blood brain barrier disruption induced by focused ultrasound and circulating preformed microbubbles appears to be characterized by the mechanical index," Ultrasound Med. Biol. **34**, 834–840 (2008).

[11]V. Sboros, "Response of contrast agents to ultrasound," Adv. Drug Delivery Rev. **60**, 1117–1136 (2008).

[12]E. Stride and N. Saffari, "Microbubble ultrasound contrast agents: A review," Proc. Inst. Mech. Eng., Part H: J. Eng. Med. **217**, 429–447 (2003).

[13]J. E. Chomas, P. Dayton, D. May, and K. Ferrara, "Threshold of fragmentation for ultrasonic contrast agents," J. Biomed. Opt. **6**, 141–150 (2001).

[14]A. Bouakaz, M. Verslius, and N. de Jong, "High speed optical observations of contrast agent destruction," Ultrasound Med. Biol. **31**, 391–399 (2005).

[15]M. Postema, A. Bouakaz, M. Verslius, and N. de Jong, "Ultrasound-induced gas release from contrast agent microbubbles," IEEE Trans. Ultrason. Ferroelectr. Freq. Control **52**, 1035–1041 (2005).

[16]J. Tu, J. Guan, Y. Qiu, and T. Matula, "Estimating the shell parameters of SonoVue microbubbles using light scattering," J. Acoust. Soc. Am. **126**, 2954–2962 (2009).

[17]T. R. Porter, C. Everbach, D. Kricsfeld, and F. Xie, "Myocardial cavitational activity during continuous infusion and bolus intravenous injections of perfluorocarbon-containing microbubbles," J. Am. Soc. Echocardiogr **14**, 618–625 (2001).

[18]W. T. Shi, F. Forsberg, A. Tornes, J. Ostensen, and B. B. Goldberg, "Destruction of contrast microbubbles and the association with inertial cavitation," Ultrasound Med. Biol. **26**, 1009–1019 (2000).

[19]C. K. Yeh and S. Y. Su, "Effects of acoustic insonation parameters on ultrasound contrast agent destruction," Ultrasound Med. Biol. **34**, 1281–1291 (2008).

[20]S. I. Madanshetty, R. A. Roy, and R. E. Apfel, "Acoustic microcavitation: Its active and passive acoustic detection," J. Acoust. Soc. Am. **90**, 1515–1526 (1991).

[21]W. S. Chen, T. J. Matula, A. A. Brayman, and L. A. Crum, "A comparison of fragmentation thresholds and inertial cavitation doses of different ultrasound contrast agents," J. Acoust. Soc. Am. **113**, 643–651 (2003).

[22]T. Giesecke and K. Hynynen, "Ultrasound mediated cavitation thresholds of liquid perfluorocarbon droplets in vitro," Ultrasound Med. Biol. **29**, 1359–1365 (2003).

[23]E. Sassaroli and K. Hynynen, "Cavitation threshold of microbubbles in gel tubes by focused ultrasound," Ultrasound Med. Biol. **33**, 1651 (2007).

[24]A. Y. Ammi, R. O. Cleveland, J. Mamou, G. I. Wang, S. L. Bridal, and W. D. O'Brien, Jr., "Ultrasonic contrast agent shell rupture detected by inertial cavitation and rebound signals," IEEE Trans. Ultrason. Ferroelectr. Freq. Control **53**, 126–136 (2006).

[25]R. O. Cleveland, O. A. Sapozhnikov, M. R. Bailey, and L. A. Crum, "A dual passive cavitation detector for localized detection of lithotripsy-induced cavitation in vitro," J. Acoust. Soc. Am. **107**, 1745–1758 (2000).

[26]A. J. Coleman, M. J. Choi, J. E. Saunders, and T. G. Leighton, "Acoustic emission and sonoluminescence due to cavitation at the beam focus of an electrohydraulic shock wave lithotripter," Ultrasound Med. Biol. **18**, 267–281 (1992).

[27]P. Marmottant, S. van der Meer, M. Emmer, M. Verslius, N. de Jong, S. Hilgenfeldt, and D. Lohse, "A model for large amplitude oscillations of coated bubbles accounting for buckling and rupture," J. Acoust. Soc. Am. **118**, 3499–3505 (2005).

[28]M. Santin, D. A. King, J. Foiret, A. Haak, W. D. O'Brien, Jr., and S. L. Bridal, "Encapsulated contrast microbubble radial oscillation associated with postexcitation pressure peaks," J. Acoust. Soc. Am. **127**, 1156–1164 (2010).

[29]A. Haak and W. D. O'Brien, Jr., "Detection of microbubble ultrasound contrast agent destruction applied to Definity®," Proceedings of the International Congress on Ultrasound (2007), Paper No. 1719.

[30]A. Y. Ammi, R. O. Cleveland, J. Mamou, G. I. Wang, S. L. Bridal, and W. D. O'Brien, Jr., "Double passive cavitation detection of Optison shell rupture," Proceedings of the IEEE Ultrasonics Symposium (2005), pp. 846–849.

[31]K. Raum and W. D. O'Brien, Jr., "Pulse-echo field distribution measurements technique for high-frequency ultrasound sources," IEEE Trans. Ultrason. Ferroelectr. Freq. Control **44**, 810–815 (1997).

[32]R. C. Preston, D. R. Bacon, A. J. Livett, and K. Rajendran, "PVDF membrane hydrophone performance properties and their relevance to the measurement of the acoustic output of medical ultrasound equipment," J. Phys. E **16**, 786–796 (1983).

[33]J. F. Zachary, J. M. Sempsrott, L. A. Frizzell, D. G. Simpson, and W. D. O'Brien, Jr., "Superthreshold behavior and threshold estimation of ultrasound-induced lung hemorrhage in adult mice and rats," IEEE Trans. Ultrason. Ferroelectr. Freq. Control **48**, 581–592 (2001).

[34]S. Podell, C. Burrascano, M. Gaal, B. Golec, J. Maniquis, and P. Melhaff, "Physical and biochemical stability of Optison, an injectable ultrasound contrast agent," Biotechnol. Appl. Biochem. **30**, 213–223 (1999).

[35]S. L. Ceccio and C. E. Brennen, "Observations of the dynamics and acoustics of traveling bubble cavitation," J. Fluid Mech. **233**, 633–660 (1991).

[36]V. A. Bogoyavlenskiy, "Differential criterion of a bubble collapse in viscous liquids," Phys. Rev. E **60**, 504–508 (1999).

[37]R. E. Apfel and C. K. Holland, "Gauging the likelihood of cavitation from short pulse, low-duty cycle diagnostic ultrasound," Ultrasound Med. Biol. **17**, 179–185 (1991).

[38]J. G. Abbott, "Rationale and derivation of MI and TI—A review," Ultrasound Med. Biol. **25**, 431–441 (1999).

[39]W. D. O'Brien, Jr., "Ultrasound-biophysics mechanisms," Prog. Biophys. Mol. Biol. **93**, 212–255 (2007).